Extensive testing on PVC sewer pipes towards identifying the factors that affect their operational lifetime

Makris, Konstantinos F.; Langeveld, Jeroen G.; Clemens, François H.L.R.

DOI
10.1080/15732479.2021.1907601

Publication date
2021

Document Version
Final published version

Published in
Structure and Infrastructure Engineering

Structure and Infrastructure Engineering

Maintenance, Management, Life-Cycle Design and Performance

ISSN: (Print) (Online) Journal homepage: https://www.tandfonline.com/loi/nsie20

Extensive testing on PVC sewer pipes towards identifying the factors that affect their operational lifetime

Konstantinos F. Makris, Jeroen G. Langeveld & François H. L. R. Clemens

To cite this article: Konstantinos F. Makris, Jeroen G. Langeveld & François H. L. R. Clemens (2021): Extensive testing on PVC sewer pipes towards identifying the factors that affect their operational lifetime, Structure and Infrastructure Engineering, DOI: 10.1080/15732479.2021.1907601

To link to this article: https://doi.org/10.1080/15732479.2021.1907601

Published online: 02 Apr 2021.

STRUCTURE AND INFRASTRUCTURE ENGINEERING
https://doi.org/10.1080/15732479.2021.1907601

Extensive testing on PVC sewer pipes towards identifying the factors that affect their operational lifetime

Konstantinos F. Makris[a], Jeroen G. Langeveld[a,b] and François H. L. R. Clemens[c,d]

[a]Department of Watermanagement, Faculty of Civil Engineering and Geosciences, Delft University of Technology, Delft, The Netherlands; [b]Partners4UrbanWater, Nijmegen, The Netherlands; [c]Department of Hydraulic engineering, Deltares, Delft, The Netherlands; [d]Faculty of Engineering, Department of Civil & Environmental engineering, Norwegian University of Science & Technology, Trontheim, Norway

ABSTRACT

Polyvinyl chloride (PVC) sewer pipes have operated for decades in a hostile environment, raising concern among sewer managers over the longevity of their drainage systems. Inspection data (CCTV and Panoramo®) reveals that severe defects have already surfaced, yet it is unknown if the material properties of PVC sewers have been affected. In order to address this issue, extensive testing (among others flexural and tensile tests, FT-IR, X-ray, viscosity measurements) was conducted on eight exhumed PVC sewer pipes (16–43 years old) with known defects and one brand-new for reference purposes. Visual examination during excavation revealed various failure causes, including uncontrolled handling of the pipes during construction or due to digging activities in the direct vicinity of the pipes. The test results indicate that physical ageing is extensively detected while other degradation mechanisms had minimal or no effect on the investigated pipes. However, mechanical testing on exhumed 3-layer pipes show that the incorporation of layered wall constructions is potentially a critical factor for the structural status of the pipe.

ARTICLE HISTORY
Received 14 October 2020
Revised 11 January 2021
Accepted 4 February 2021

KEYWORDS
Ageing; degradation; inspection; plastic pipes; polymer testing; PVC; sewers

1. Introduction

Over the past decades, Polyvinyl Chloride (PVC) has become one of the dominant construction materials in urban drainage systems, as well as for drinking water and gas distribution networks, due to the material's light weight and/or resistance against many corrosion processes. This fact has led to numerous studies concerning the structural integrity and chemical resistance of PVC piping systems. Research on exhumed gravity PVC sewer pipes suggests that there are no signs of impoverished physical and mechanical properties (Alferink, Guldback, & Grootook, 1995; Bauer, 1990; Folkman, 2014; Whittle & Tennakoon, 2005).

Furthermore, testing of a series of chemicals usually found in sewers (i.e. H_2SO_4, Na_2SO_4, NaOH, NaClO-Cl_2, ClO_2) on PVC pipes has led to the conclusion that no significant chemical alterations in PVC composition are observable (Bishop, 1990; Fumire, 2008; Hawkins & Mass, 1994; Lasfar et al., 2014). Concerning the elastomeric joints, only extreme values of bending (>10°) and deflection (>36%), or the complete pull-off could result in leakages (Arsénio, 2013; Meijering, Wolters, & Hermkens, 2004). Therefore, based on scientific literature, PVC piping systems seem to be almost inert to chemical interactions, encouraging several researchers (Folkman, 2014; Meerman, 2008; Whittle & Tennakoon, 2005) to express their expectation for an exceptional operational lifetime of at least 100 years.

Nonetheless, the issue of PVC pipes performance has lately gained the attention of sewer managers, as PVC pipes occupy large parts of urban drainage systems and the operational lifetime of many PVC pipes is already over four decades. Although this concern could be attributed to the misled notion of directly linking the (technical) status of a pipe with its age (Stanic, Langeveld, & Clemens, 2012; Stone et al., 2002), it seems to be verified in practice. CCTV and Panoramo® inspection data unambiguously indicate that all kinds of known defects already occur and they even evolve at a relatively fast pace (Makris, Langeveld, & Clemens, 2020). Additionally, due to the inspector's subjectivity and the exclusive inspection of the inner pipe surface, the results of CCTV inspections are prone to errors and show a significant uncertainty. As a result, it is likely that there is high contingency of undetected defects being present (Dirksen et al., 2013).

The present study aims at exploring this discrepancy between scientific research and observations in practice, by discussing the durability of eight PVC sewer pipes (that have been in operation) with known defects, which were excavated and subjected to a range of tests and analyses. The results of such comprehensive testing offer the

CONTACT Konstantinos F. Makris k.makris@tudelft.nl Department of Watermanagement, Faculty of Civil Engineering and Geosciences, Delft University of Technology, Stevinweg 1 (Building 23), Delft, 2628CN The Netherlands

opportunity to conclude on potential degradation and the overall performance of the examined pipes, while indicating prerequisites for establishing future sewer asset management strategies.

2. Materials and methods

2.1. Pipe samples

Eight operating PVC pipes, incorporated in municipal wastewater systems, were exhumed in cooperation with the municipalities of Almere and Breda. The pipes were selected based on the year of installation, the existing defect(s) and the feasibility of excavation. The length of the excavated pipes was approximately one meter of unaffected material in addition to the length that included the developed defect. A brand-new, obtained directly after being produced, PVC pipe was also included in the study in order to serve for reference purposes. The main characteristics of the tested pipes are presented in Table 1.

Pipes A-3 and A-4 are perforated across the longitudinal axis forming a void core, while pipes B-3 and B-4 are 3-layer pipes having a recycled PVC and a foamed core respectively. The remaining pipes are produced with a single PVC layer. Figure 1 presents the inspection images of the pipes which suffered from a structural defect. Concerning pipes B-1 and B-4, the detected defect was root penetration which occurred via elastomeric connections, the integrity of which is not assessed in the current work. Therefore, these pipes had no visually detected defects, except for scratches which were present on all excavated pipes and were inflicted most likely during installation and/or exhumation, although appropriate care was taken regarding the latter.

2.2. Analyses

Several tests were conducted in order to identify the main physical, chemical and, relatedly, mechanical properties of the samples. Additionally, information about the pipe production process was obtained by certain analyses, in an effort to explore the possible correlation between the production method, choice of materials and the properties of the pipes.

2.2.1. Determination of physical properties

Quantification of physical properties included the estimation of density and intrinsic viscosity of the examined samples. The density of the pipes was estimated by immersing samples in distilled water (ISO 1183-1, 2012, Method A). The masses of the dry sample and the displaced water were measured (Mettler Toledo PG2002-S balance), as well as the water temperature (Testo 104-IR thermometer). Subsequently, the volume of each sample was estimated, resulting in the determination of density.

The chain lengths of polydisperse polymers (like PVC) were assessed via their intrinsic viscosity, which represents the resistance against internal flow. Intrinsic viscosity was estimated by following a series of steps based on the use of a rheometer (Anton-Paar MCR 302). The rheometer was equipped with a concentric cylinder (40.018 mm effective bob length, 26.663 mm bob diameter) and a measuring cup (diameter: 28.920 mm). The investigated solutions were prepared by dissolving PVC samples of various weights (ranging from 100 to 250 mg) in 50 mL cyclohexanone (vapor pressure 3.4 mmHg at 20 °C, assay $\geq$99.5%) at 80 ± 5 °C, in Erlenmeyer flasks equipped with stoppers (ASTM D2857-16, 2016).

A Mettler Toledo xs205 balance and a Thermo Fisher 4500 pipette were utilized for measuring the weight of the samples and the volume of the solver, respectively. Subsequently, the polymer solutions were rested at ambient temperature for at least 45 minutes. After filtering (0.45 μm Whatman discs) in order to remove the inorganic elements, each solution was introduced in the rheometer, resting at the temperature chamber for 30 minutes at 20 °C. Finally, the viscosity was measured at shear rates ranging from 1 to 250 s^{-1} at 1 s^{-1} steps, allowing 10 seconds at each shear rate to stabilize (pre-shearing). The described testing protocol was established after numerous trials, striving towards a consistent measuring technique with lower measuring uncertainties.

The intrinsic viscosity at each shear rate was acquired via multi-concentration measurements by extrapolating the inherent viscosity (Equation (1)) to zero concentration (Kraemer, 1938). Finally, the zero-shear intrinsic viscosity has to be estimated by extrapolating to the theoretical zero-shear point:

$$\eta_{inh} = \ln\left(\frac{\eta}{\eta_o}\right) \Big/ c \tag{1}$$

where η_{inh} is the inherent viscosity (mL/g), η is the solution's viscosity (Pa·s), η_o is the solver's viscosity (Pa·s) and c is the polymer solution concentration (g/mL).

2.2.2. Thermal analyses

Differential Scanning Calorimetry (DSC) is a thermal analysis which detects the fluctuations in the required heat flow, so that the temperature of the tested samples increases at a specific rate. DSC reveals the major thermal transitions, i.e., the glass transition temperature (T_g) and the processing temperature (Tc). A DSC device (Perkin Elmer 8500) supplied the samples with heat from ambient temperature to 250 °C at a 10 °C/min rate under a nitrogen gas atmosphere flowing at 20.0 mL/min (similar to ISO 18373-1, 2007). For this analysis, four samples (10 mg approximately) per pipe were tested, being sealed in Perkin Elmer standard aluminum sample pans and covers.

An additionally utilized thermal technique is Thermo-Gravimetric Analysis (TGA), in which the weight is measured as a function of the temperature of the specimen, which is increased at a specific rate (ISO 11358-1, 2014). This analysis shows the onset and rate of thermal degradation, as well as the residual content of inorganic elements (stabilizers, fillers or impurities). For this purpose, one sample per pipe was tested in a TGA instrument (Perkin Elmer 4000), at a temperature range from ambient to 600 °C at 10 °C/min rate under a nitrogen gas atmosphere (20.0 mL/min).

Table 1. Characteristics of sewer PVC pipes used for analyses.

Sample	Installation area	Installation year	Excavation year	DN	Embedded Core	Soil	Surface	Mean soil cover (m)	Defect (EN 13508-2)
A-1	Almere (NL)	1976	2019	250	–	Clay	Paved path	1.55	Crack at the connection (BAF)
A-2		1977		250	–		Paved street	2.32	Deformed at crown (BAF)
A-3		1978		250	Void		Paved path	1.52	Pointy break at side (BAF)
A-4		1980		250	Void		Paved street	1.51	Crack at bottom (BAB)
B-1	Breda (NL)	1977	2018	250	–	Sand	Paved street	1.55	Root intrusion (BBA)
B-2		1979		250	–		Paved street	1.30	Break (BAC)
B-3		1995		200	Recycled		Paved street	1.58	Complicated crack (BAB)
B-4		2002		160	Foamed		Soil	1.16	Root intrusion (BBA)
R(new pipe)	–	–	–	250	–	–	–	–	–

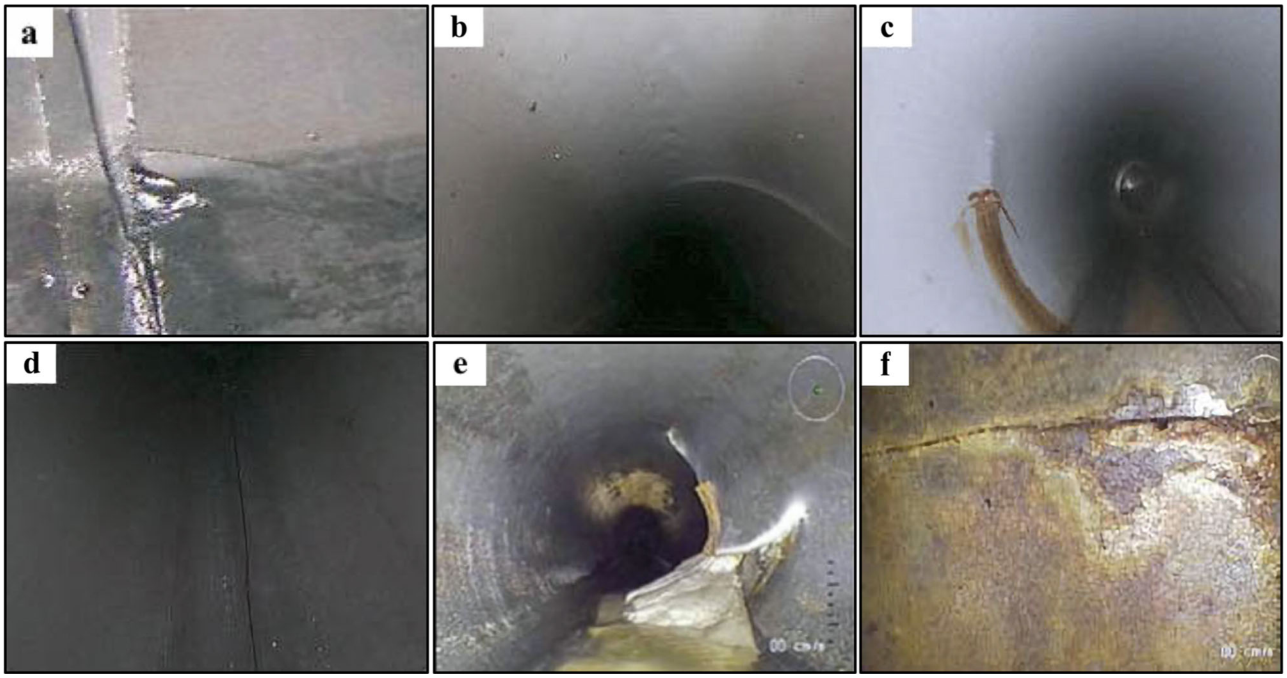

Figure 1. CCTV or Panoramo® footage of: (a) Exhumed pipe A-1 (DN 200, 43 years old) with crack at the connection. (b) Exhumed pipe A-2 (DN 200, 42 years old) with deformed top. (c) Exhumed pipe A-3 (DN 200, 41 years old) with pointy break at the side. (d) Exhumed pipe A-4 (DN 250, 39 years old) with crack at the bottom. (e) Exhumed pipe B-2 (DN 250, 39 years old) with break. (f) Exhumed pipe B-3 (DN 200, 23 years old) with complicated crack.

2.2.3. Spectrometric and microscopic measurements

In order to directly detect chemical degradation of the pipe material, a Perkin Elmer Spectrum 100 device supplied with an ATR (Attenuated Total Reflection) crystal was used within a wavenumber range of 4000 to 550 cm^{-1}. With the aid of infrared spectroscopy, the molecular motions which are not attributed exclusively to the composition of PVC can be tracked, indicating potential chemical alterations. Moreover, X-Ray Fluorescence (XRF) analysis was utilized in order to detect the existence and concentrations of inorganic elements which are present within the composition of the examined pipe samples. The measurements were conducted with a Panalytical Axios Max WD-XRF spectrometer and data evaluation was implemented with the aid of SuperQ5.0i/Omnian software.

Finally, a Scanning Electron Microscope (SEM, JEOL JSM-7500F) configured with secondary and backscattered electron detectors was used. The microstructure was observed by SEM, providing information for identifying the likely failure cause(s) (e.g. cavities) of the specimens subjected to tensile tests. Energy Dispersive X-ray Spectroscopy (EDS) during SEM has been applied to detected inherent defects, obtaining information about the elemental composition of failure areas and the processing quality.

2.2.4. Tensile and flexural testing

The results of mechanical testing incorporate any type of present degradation, as well as production quality and installation quality. Furthermore, while for other conducted analyses the material properties were traced with very small samples or surface analyses, the tensile and flexural testing specimens were milled from the whole pipe thickness. Therefore, the complete structural composition of the pipes was considered.

Flexural tests were conducted with a Zwick Universal Testing Machine of 20 kN load cells combined with a four-point bending set-up on five specimens per pipe which were milled along the longitudinal direction at the crown of each pipe. Depending on the thickness of each pipe, the displacement rate varied from 11 to 15 mm/min in order to achieve 5 mm/mm maximum strain in the outer fibres of the specimens (ASTM D6272-17, 2017).

Although flexural tests activate similar mechanisms found at unpressurized pipes within soil (in particular deflection),

Table 2. Main physical properties of examined PVC pipes.

Sample	Density (g/cm^3)	Intrinsic viscosity (mL/g)
A-1	1.42 ± 0.00	128.26 ± 3.87
A-2	1.41 ± 0.00	128.47 ± 1.93
A-3	1.41 ± 0.01	128.94 ± 1.99
A-4	1.41 ± 0.01	128. 17 ± 1.76
B-1	1.41 ± 0.01	124.49 ± 1.48
B-2	1.41 ± 0.01	128.78 ± 1.46
B-3	1.41 ± 0.01	*
B-4	1.49 ± 0.01	85.21 ± 0.92
R	1.41 ± 0.01	120.74 ± 1.13

*Pipe not tested due to equipment failure.

tensile testing is mainly found in the literature (Alferink et al., 1995; Bauer, 1990; Whittle & Tennakoon, 2005), as it is discussed later-on in this article. Therefore, uniaxial tensile tests were complementarily performed only on the pipes which were firstly excavated (B-1, B-2, B-3 and B-4) and the reference pipe (R). Tensile testing was conducted with a Zwick Universal Testing Machine (20 kN load cells) at 5 mm/min displacement rate on 10 specimens per tested pipe. The specimens were milled from various circumferential positions along the longitudinal direction based on ISO 6259-2 (1997, Type 1). The ultimate tensile stress and elongation at break were determined in order to track the degree of physical ageing and assess the effect of potentially compromised physical or chemical properties.

3. Results

The values of density and intrinsic viscosity of the tested samples are summarized in Table 2. The majority of the pipes demonstrate similar values, close to the reference pipe R. A lower intrinsic viscosity value is distinguished only regarding pipe B-4.

The process followed in order to estimate the intrinsic viscosity is illustrated in Figures 2 and 3. The relationship between inherent viscosities and solution concentrations is fitted using linear regression (Figure 2). Linear extrapolation to zero concentration provides the intrinsic viscosity for each tested shear rate. This procedure was repeated for the considered shear rates, whose selection has been derived by the conducted uncertainty analysis for rheometric measurements with Anton-Paar 302 (Appendix). Additionally, the shear-dependent intrinsic viscosities can be also described by a linear fit (Figure 3), which allows the extrapolation to the zero-shear rate and the estimation of the respective intrinsic viscosity.

The results obtained from the thermal analyses are presented in Table 3. The glass transition temperature (T_g) is obtained by the DSC curve as shown in Figure 4 (left). All pipe samples demonstrate a glass transition temperature within the range of 81.6–83.7 °C with onset temperature values of the rubbery state within 79.2–81.4 °C (Table 3). The point between the two endotherms (ΔHa & ΔHb) reveals the production process temperature (T_c). ΔHa and ΔHb signify the melting of secondary and primary crystallites respectively. Processing temperature varied between 169.3–179.9 °C for pipes manufactured before 1980, whereas newer PVC pipes (after 1995) were processed at a temperature range of 185.7–192.4 °C.

The curves derived by TGA (Figure 4, right) indicate two characteristic decomposition temperature points [Primary (T_{onset}) and Secondary (T_{SD}) Decomposition Temperature]. T_{onset} denotes commencement of dehydrochlorination and volatile components loss, and T_{SD} reveals the starting point of scission of the main polymer chains back-bone. The plateau formed at the end of the analysis represents the amount of inorganic elements in the PVC matrix, which required additional thermal energy to decompose. The characterization of the thermal stability of the investigated samples was finalized by detecting the points of Maximum Rate of Decomposition Temperature (MRDT) on the weight curve (inflection points in the respective first derivative). All pipe samples show values of T_{onset}, T_{SD} and MRDT in close proximity, while the concentration of residual content of non-volatile inorganic elements differs (15.3–26.6%).

Elemental analysis via XRF (Table 4) revealed 15 different inorganic elements, the majority of which were present in all pipe samples in various concentrations. Three main types of inorganic elements were justifiably present, as they contribute to the production process of PVC pipes in the form of stabilizers, fillers and pigments. For piping applications, lead (Pb) based stabilizers were used until early 2000s in Europe (Anders, 2014), predominantly tribasic lead sulphate ($3PbO{\cdot}PbSO_4{\cdot}H_2O$), dibasic lead stearate [$2PbO{\cdot}Pb(OOC\text{-}C_{17}H_{35})_2$] and normal lead stearate [$Pb(OOC\text{-}C_{17}H_{35})_2$] (Wilkes, Summers, Daniels, & Berard, 2005). The transition from Pb to zinc (Zn) based stabilizers due to high toxicity of Pb was tracked among the old and reference pipes. Common mineral fillers are calcium carbonate ($CaCO_3$), kaolin ($Al_2O_{32}SiO_{22}H_2O$), talc [$Mg_3SiO_{10}(OH)_2$], mica [$K_2Fe(Al_2Si_6O_{20})(OH_4)$], wollastonite ($CaSiO_3$), barite ($BaSO_4$) and calcium sulphate ($CaSO_{22}H_2O$). Pigments ($TiO_2$) are introduced in order to enhance color weatherability. Other present inorganic elements derive from introduced clay minerals, namely Al, Fe, Mg, Ba, K, Ca, and Sr (Wilkes et al., 2005).

Figure 5 presents the results from FT-IR analysis. Peaks of considerable intensity level within the investigated spectrum were found and could be interpreted according to known molecular motions (Jakubowicz & Möller, 1992; Noda, Dowrey, Haynes, & Marcott, 2007; Wypych, 2015). The examined reference pipe demonstrated peaks at the same wavelengths as the old ones. In detail, these peaks appeared at circa 2970 cm^{-1} (CH stretch next to Cl), 2913 cm^{-1} (CH_2 asymmetric stretch), 1427 cm^{-1} (CH_2 wag), 1354 cm^{-1} (CH_2 wag), 1255 cm^{-1} (CH bend), 1100 cm^{-1} (C-C stretch), 960 cm^{-1} (CH_2 rock), 876 cm^{-1} ($CaCO_3$), and 687 cm^{-1} (C-Cl stretch).

Discrepancies in the intensity levels among different samples are mainly caused by the high sensitivity of the applied method, especially since the tested samples were rigid and slightly curved instead of fine powder, inhibiting absolute crystal contact. Peaks at the same wavelengths were observed irrespectively of the tested surface (i.e. interior, exterior and middle of pipe thickness). Besides expected peaks, small abnormalities at wavelengths 1711 and/or 1739 cm^{-1} were found during testing on the exterior of exhumed pipes, indicating the existence of carbonyl groups

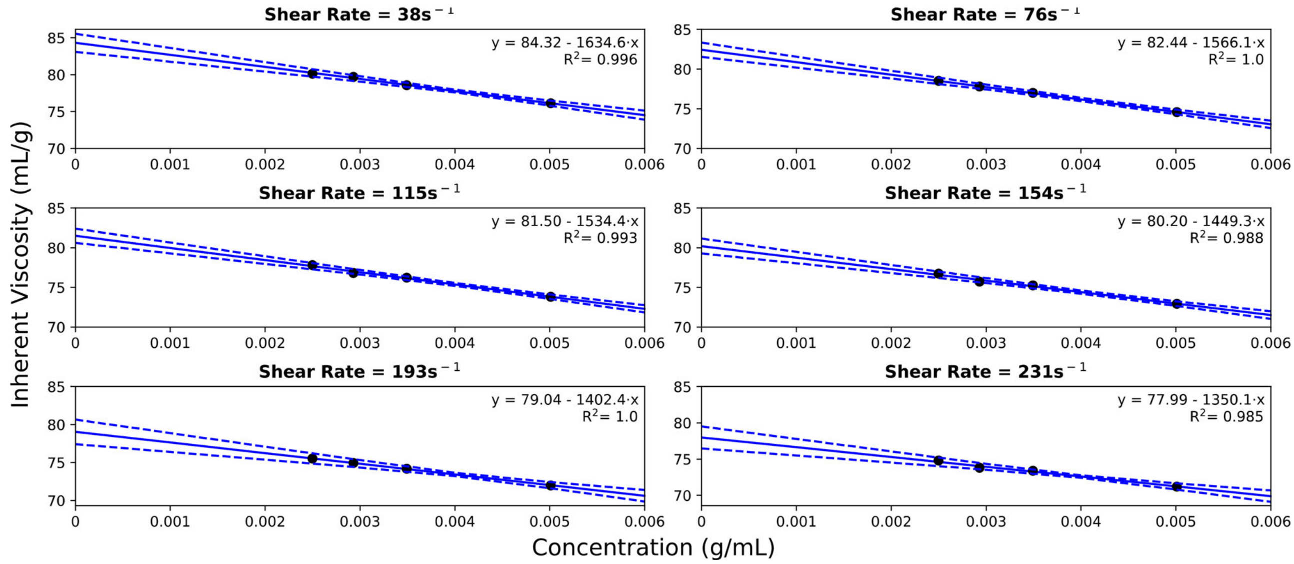

Figure 2. Inherent viscosity with respect to solution concentrations of pipe B-4 for shear rates of lowest uncertainties. The value of the intrinsic viscosity for each shear rate is obtained by extrapolation of the linear regression fit to zero concentration (e.g., 84.32 mL/g for shear rate 38 s^{-1}).

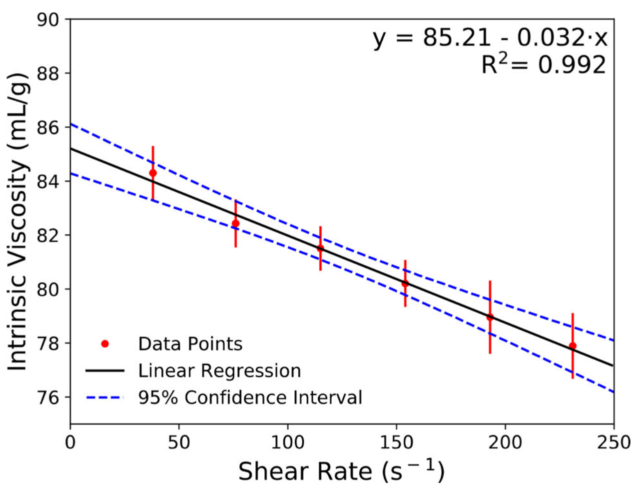

Figure 3. Intrinsic viscosity with respect to shear rates of lowest uncertainties for pipe B-4. The values of the intrinsic viscosity are obtained by Figure 1. The zero-shear intrinsic viscosity is estimated by extrapolation of the linear regression fit to zero shear rate (i.e., 85.21 mL/g).

(Matuana, Kamdem, & Zhang, 2001; Wypych, 2015). Depending on the installation area, the pipes demonstrated different peaks at 1711 cm^{-1} (Figure 5, upper) and 1739 cm^{-1} (Figure 5, lower).

Tensile testing indicated high variability among different pipes (Figure 6). Concerning single layer PVC pipes (B-1 & B-2), a translation was observed towards higher ultimate stress, higher E-modulus and lower strain at break values, compared to the reference pipe. Nonetheless, elongations at break remained high (136.9 ± 44.1% for pipe B-1 and 175.3 ± 20.1% for pipe B-2). Regarding pipe B-3, with a recycled core, the average ultimate tensile stress was in proximity to the reference pipe although break occurred earlier. Pipe B-4, incorporating a foamed core, showed the lowest values of ultimate stress and strain at break. Variations between samples from the same pipe may have originated due to the wide range of temperature (±2 °C) at which tensile testing was performed, rising the testing uncertainties, as depicted by the respective standard deviations.

In the explored specimens, two cases of premature failure during tensile testing, samples B-1 and B-3 at 53.4% and 23.4% elongation respectively, were analyzed with SEM. Magnification of the cross-sections at break revealed that both failures were initiated due to cavities within the structure (Figure 7). Especially concerning sample B-3, numerous cavities were found in the recycled core and, in particular, near the interface between virgin and recycled PVC (Figure 7, right). Chemical analysis via EDS indicated that no foreign elements were traced at the inspected areas.

Flexural testing revealed that the same pattern as in tensile testing exists for single layer pipes, with older pipes demonstrating higher values of ultimate flexural strength

Table 3. Values obtained by differential scanning calorimetry and thermo-gravimetric analysis for the examined pipes.

	DSC			TGA				
Sample	Tonset (°C)	Tg (°C)	T_c (°C)	Tonset (°C)	MRDT1 (°C)	TSD (°C)	MRDT2 (°C)	Wt (%) at 600 °C
A-1	80.0	82.4	174.1	288.8	296.4	451.9	476.3	21.1
A-2	79.8	83.1	169.3	290.2	301.8	448.3	474.7	18.4
A-3	79.6	82.0	174.7	288.4	303.4	443.2	478.1	17.9
A-4	79.2	81.6	175.1	287.3	296.4	450.1	479.9	19.5
B-1	79.4	82.5	179.8	290.8	305.4	436.5	472.3	15.3
B-2	81.4	83.4	179.9	290.4	299.7	438.2	481.3	16.8
B-3	80.8	83.2	185.7	292.0	303.2	435.0	474.6	17.2
B-4	81.2	83.7	192.4	291.4	304.4	439.7	476.7	26.4
R	80.6	83.1	185.7	286.7	301.2	442.6	479.4	19.6

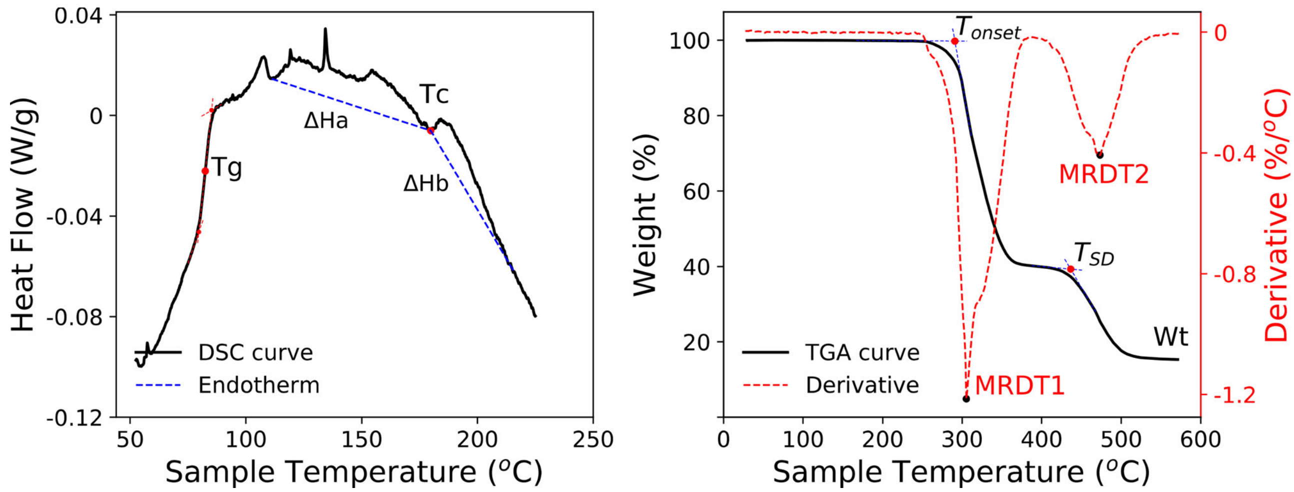

Figure 4. Left: Curve obtained via Differential Scanning Calorimetry on pipe B-2 including indication of glass transition (Tg), processing temperature (Tc) and endotherms ΔHa and ΔHb. Right: Curve obtained via Thermo-Gravimetric Analysis on Pipe 5 and the respective derivative (dashed line) including indication of temperature of thermal degradation onset (Tonset), of maximum degradation rates (MRDT1 & MRDT2), and residual inorganic elements (Wt).

Table 4. Elemental composition (Wt % · 10-3) of the examined pipes derived from XRF analysis.

Sample	Al	Ba	Bi	Ca	Fe	K	Mg	P	Pb	S	Si	Sr	Ti	Zn	Zr
A-1	52	–	4	1908	17	18	25	9	1268	311	112	3	49	–	–
A-2	33	–	6	1499	13	–	25	3	1302	98	91	4	61	–	–
A-3	91	–	–	1457	48	39	33	10	1396	77	286	2	42	–	5
A-4	61	–	–	1444	17	20	21	3	1401	162	122	3	52	–	5
B-1	6	14	–	554	–	–	15	2	852	174	19	1	68	–	–
B-2	8	–	–	677	–	–	16	1	729	130	19	–	25	–	–
B-3	29	–	–	1165	12	5	20	2	783	104	99	4	42	–	–
B-4	37	58	–	4369	19	10	24	7	1045	87	178	10	8	–	–
R	95	–	–	1570	4	11	63	2	–	5	92	3	111	1	–

and flexural modulus compared to the reference pipe (Figure 8). However, high variability was noticed in some cases among samples coming from the same pipe, especially regarding pipe B-1. Further, pipe B-4 showed relatively low values in terms of flexural stress but similar to single layer pipes in terms of flexural modulus. On the contrary, pipes with a void core (A-3 & A-4) exhibited the lowest flexural modulus values. Pipe B-2 was not tested due to insufficient material. The average values of the tensile and flexural properties for each pipe are presented in Table A1 in the Appendix.

4. Discussion

4.1. Extent of degradation on exhumed pipes

A series of material tests were conducted based on methods described in scientific literature particularly for PVC pipes (Makris et al., 2020). Since material properties are influenced by several factors, comprehensive testing was necessary in order to identify how physical ageing interacts with potential chemical and mechanical degradation. Table 5 presents a comparison between the acquired properties and those dictated in NEN-EN 1401-1 (2019) for new non-pressure PVC pipes. The required parameter values for new pipes denote the threshold above which the initial properties should be, but their actual values still remain unknown.

Measurements of physical properties showed that the density values of the investigated pipes were similar and within the expected range for PVC (Cardarelli, 2008; Orwoll, 2007) and new PVC sewer pipes (Table 5). The fact that the density of older pipes is not higher than the newer ones as expected (Hutchinson, 1995) implies that physical ageing is not so clearly detected via density measurements as with other methods (e.g. tensile testing). Intrinsic viscosity of pipe B-4 proved to be noticeably less when compared to the rest of tested pipes, which was a precursor of lower tensile properties, although the embedded foamed core seemed to be of higher significance. Nonetheless, lower values of intrinsic viscosity may be yielded due to removing higher order molecules during filtering.

No distinct signs of degradation were detected via thermal analyses. The magnitude of glass transition temperature (T_g) is likely to decrease as degradation proceeds (Hamid, Amin, Maadhah, & Al-Jarallah, 1992), while the same tendency is expected for the characteristic temperature values (T_{onset} and T_{SD}) derived by TGA. Nonetheless, all the investigated pipes demonstrated values relatively close to the reference one, being similar to those of unaffected pipes (Fumire, 2008). Moreover, the degree of gelation is usually assessed based on the area of the two endotherms observed in the DSC graphs (Gramann, Cruz, & Ralston, 2010; Real, João, Pimenta, & Diogo, 2018). However, this process was not conducted in the current study due to uncertainties of the applied method (i.e. sample preparation and variations through the pipe thickness) and the limited number of tested samples (maximum 4). In addition, a clear connection between the level of gelation assessed with the mentioned methods and the performance of PVC pipes does not seem to prevail (Alferink et al., 1995; Real et al., 2018).

XRF analysis indicated that certain elements, which constitute common stabilizers, fillers and pigments for PVC pipes (Wilkes et al., 2005), were found in all samples. At the same time, PVC proved to be a polydisperse material with various elemental compositions. Discrepancies were detected even in pipes which originate from the same production

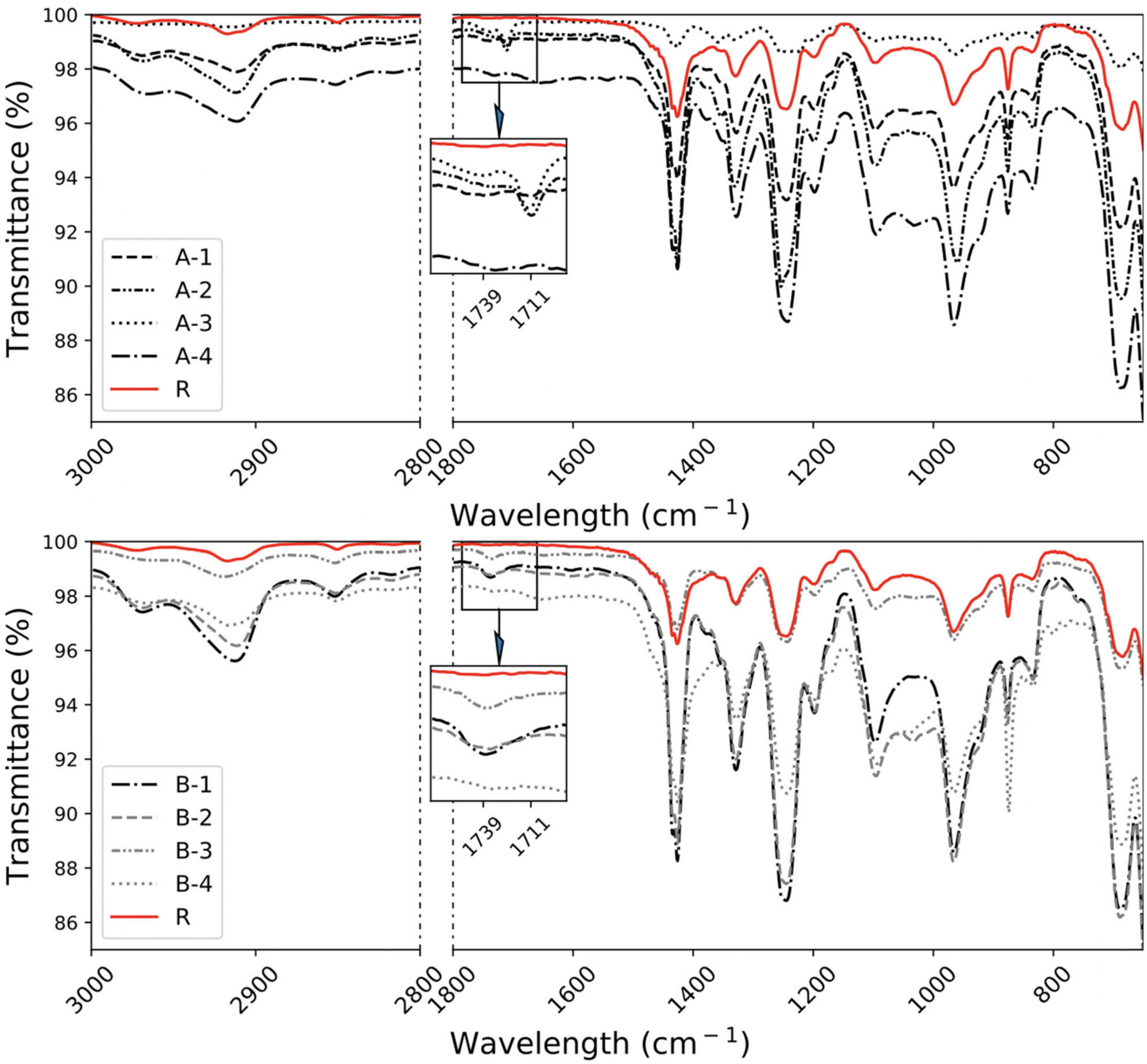

Figure 5. FTIR-ATR transmittance spectra of the exterior of examined pipes from Almere (upper graph) and Breda (lower graph). Only wavelengths with peaks are displayed. The wavelengths that denote carbonyl groups are magnified in built-in graphs.

period and manufacturing company, such as pipes B-1 and B-2. However, it should be stressed that XRF is mainly a surface analysis as it penetrates only 2–20 μm within the material. The variability in the type and concentration of inorganic elements combined with the range of processing temperatures revealed the disparate processing procedures followed by different manufacturers and through separate production periods. Only recently produced pipes (B-3, B-4 and R) obey to the levels of required processing temperature for PVC sewer pipes, while most pipes (except for A-1 and B-4) have the required level of PVC content (Table 5). These factors are generally expected to result in varying pipe properties and quality levels (Weller, Hermkens, & Van der Stok, 2016).

The main compositional structure of PVC seems to be intact (Noda et al., 2007), albeit the detected peaks at 1711 and 1739 cm^{-1} in the FTIR graphs indicate oxidation expressed via the existence of carbonyl functional groups on several pipes (Hamid et al., 1992). The fact that similar results were found also at the external surface of water distribution PVC pipes in another study (Kowalska, Rudawska, & Kowalski, 2014), leads to the speculation that certain soil parameters potentially affect the chemical stability of PVC material. Additionally, the pipes manifested discolorization, an indication of dehydrochlorination, at several points of the outer surface and at the inner bottom surface at the area of sewage flow. Nonetheless, discolorization was definitely limited at the surface level while overall testing on discolored specimens proved that material properties were not affected.

Furthermore, tensile tests showed a variability between pipes, as a consequence of the pipes' age and the construction materials. There was an evident indication of physical ageing regarding single layer pipes, as a transition was observed towards higher ultimate stress and modulus values, followed by lower strains at break. These values were of

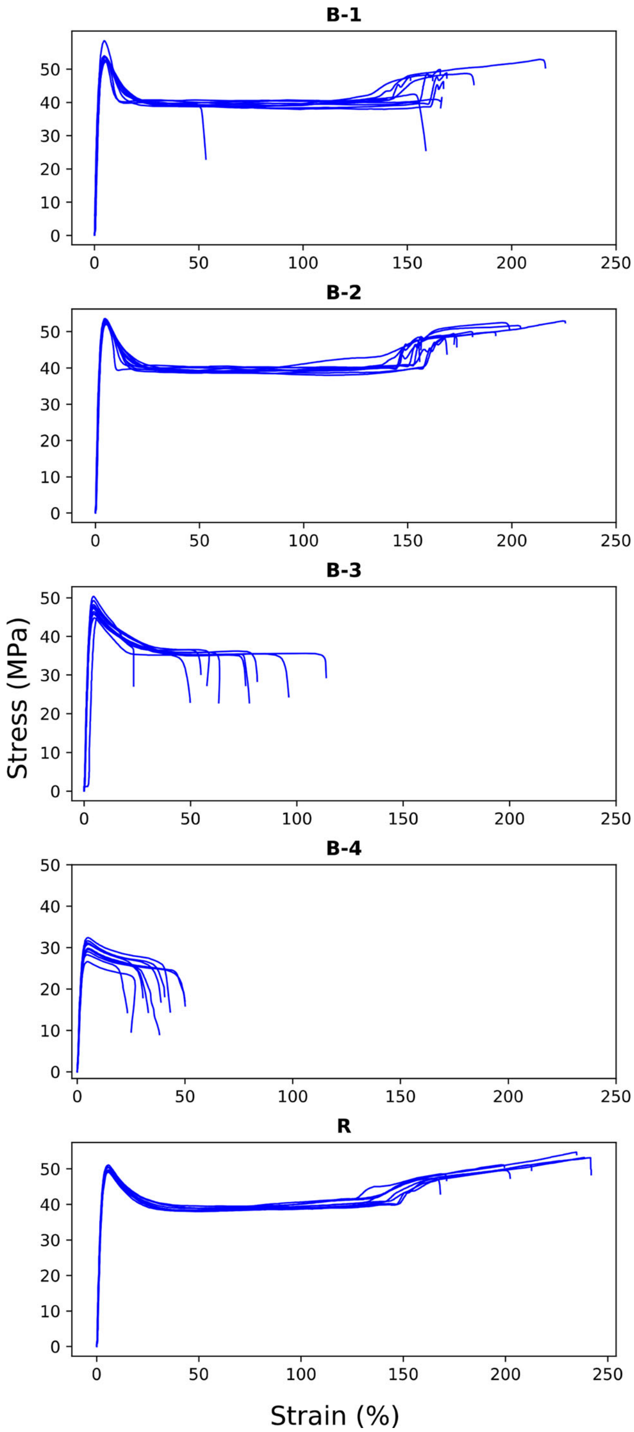

Figure 6. Stress – Strain curves derived by uniaxial tensile testing on five specimens of pipes: B-1 (41 years, DN 250), B-2 (39 years, DN 250), B-3 (23 years, DN 200 with a recycled core), B-4 (16 years, DN 160 with a foamed core), and R (new pipe). Displacement rate = 5 mm/min. Testing temperature = 24 ± 2 °C.

similar or higher magnitude compared to old PVC sewer pipes investigated in other studies (Alferink et al., 1995; Bauer, 1990; Whittle & Tennakoon, 2005). Ductility of old pipes was found to be reduced but still remained at high levels.

However, it has to be stressed that service temperatures can be lower than the tested ones, resulting in a more brittle behaviour and a reduced capacity of the pipe to absorb energy before fracturing (McGarry, Mandell, & Hsueh-Lee, 2007; Scholten, van der Stok, Gerets, Wenzel, & Boege, 2016; Visser, Bor, Wolters, Warnet, & Govaert, 2011). It is expected that, after a certain point, this brittleness will potentially cause issues concerning the pipe inspection and the placement of new household connections. Moreover, incorporation of cores led to a decrease in all tensile properties, yielding lower values of elongation at break than required (Table 5). SEM indicated that more cavities are prone to be created in pipes with embedded cores, although a noticeable cavity was also found to be responsible for the failure of a sample of a single layer pipe (B-1). Consequently, poor installation quality or differential ground sedimentations could be critical factors as excessive tension of such pipes could lead to premature failures.

Four-point flexural testing was considered as more appropriate than tensile testing in order to describe the stress conditions of gravity sewers in the ground. In addition, the flexural modulus is highly correlated with ring stiffness, as follows (Moser & Folkman, 2008):

$$SN = \frac{E \cdot I}{D^3} \tag{2}$$

where SN is the ring stiffness (N/m/m), E is the modulus of elasticity (Pa), I is the moment of inertia of pipe wall per unit length (m^4/m) and D is the mean diameter (m).

Ring stiffness is an important parameter for gravity flow pipes as it is a measure of resistance against deflection (Equation 3) and its estimation is used for the design and classification of thermoplastic pipes (ISO 9969, 2016). Since the available lengths of unaffected pipe segments were not sufficient to perform ring stiffness tests, flexural tests were preferred in order to estimate and compare the modulus of elasticity of the tested pipes. However, deriving actual values for ring stiffness of a cross-section via the obtained E modulus values would be assigned with substantial uncertainties, given that the samples were not taken from the whole cross-section:

$$SN = \left(0.0186 + 0.025 \cdot \frac{y}{d}\right) \frac{F}{L \cdot y} \tag{3}$$

where SN is the ring stiffness, y is the deflection (m), d is the average inside diameter, F is the applied force (N) and L is the length of the test piece (m).

Results from flexural tests revealed that a foamed or recycled core did not affect the performance against bending, yielding similar results with single layer pipes. However, pipes with a void core (A-3 and A-4) demonstrated lower flexural modulus values. While several factors may have led to this outcome (for instance soil composition, backfill quality, traffic load), samples from these pipes performed at the same level in a series of tests (density, intrinsic viscosity, thermal analyses) as single layer pipes subject to similar conditions (A-1, A-2). Therefore, the presence of the void core is considered as the main parameter for lower flexural properties. It should also be emphasized that both tensile and flexural testing on different samples of single layer pipe B-1 showed high variability, denoting high heterogeneity levels within the pipe.

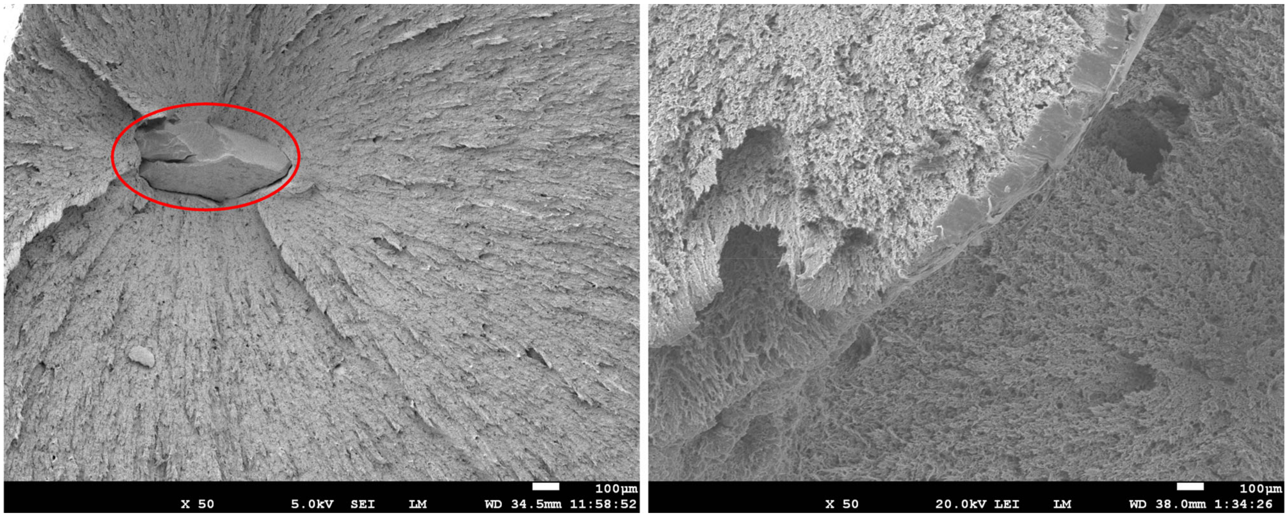

Figure 7. Images obtained via Scanning Electron Microscope at prematurely failed cross-sections during tensile testing for samples of B-1 (left) and B-3 (right). The cavity found in B-1 sample (within red circle) is covered with the coating material needed for this analysis.

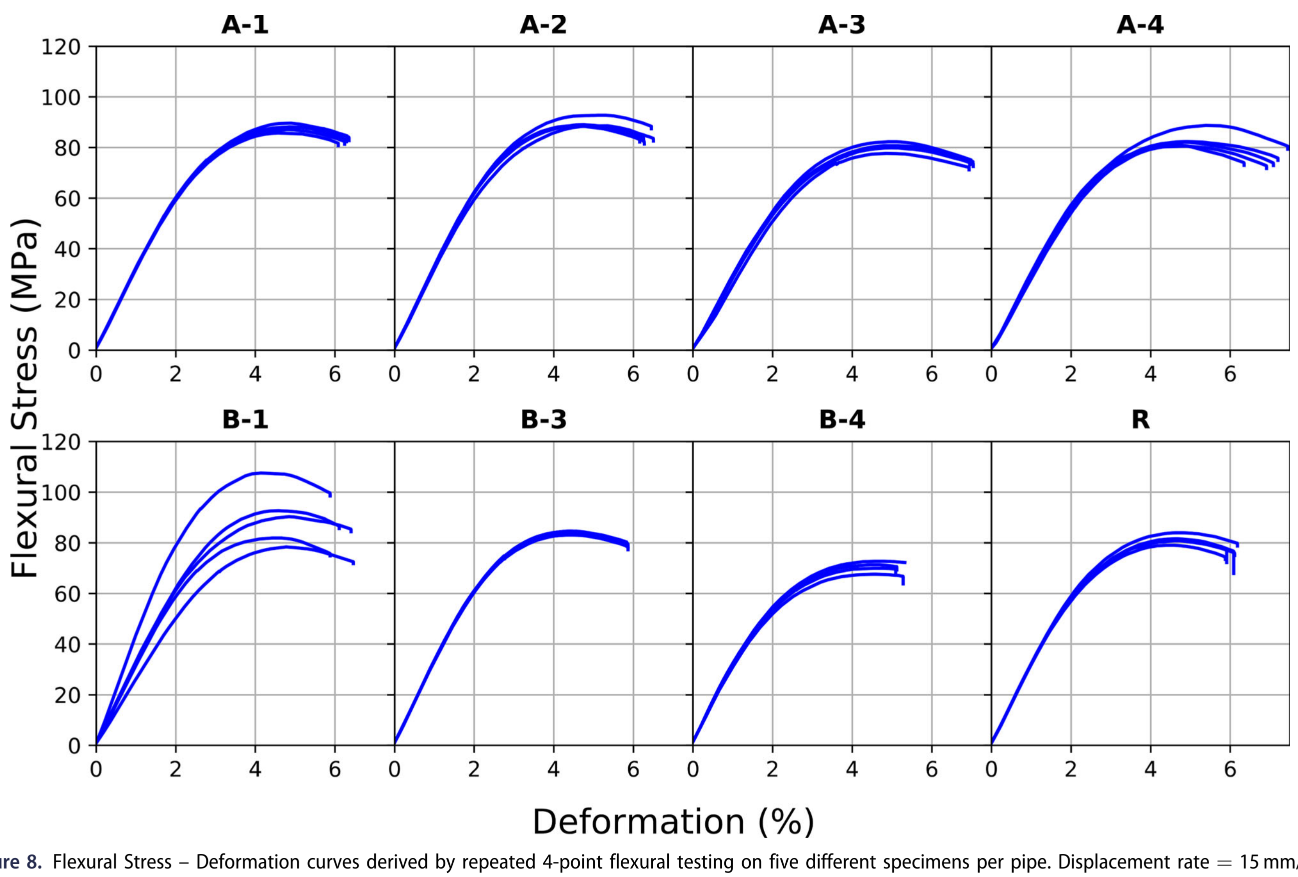

Figure 8. Flexural Stress – Deformation curves derived by repeated 4-point flexural testing on five different specimens per pipe. Displacement rate = 15 mm/min (B-3: displacement rate = 14 mm/min, B-4: displacement rate = 11 mm/min). Testing temperature = 20 ± 0.2 °C.

4.2. Causes of pipe failure

Investigation of material properties provided sufficient information about the structural integrity of the affected pipes, without justifying the origins of the occurred failures. The actual causes were exposed either during excavation or via careful interpretation of inspection data. The cause of failure of pipe A-1 could be attributed to joint bending. Inspection footage clearly indicated angular bending at the joint (Figure 1(a)) leading to the development of contact points between the pipes. Such contact points impose excessive bending moments and local peaks in tensile stresses on the pipe during operation. This state may have initiated by poor installation quality and/or differential soil sedimentation (Arsénio, 2013), a known phenomenon at the installation site due to the type of native soil (clay).

Settling conditions and/or poor soil compaction are considered as a plausible justification also for the deformed top observed in pipe A-2. This pipe was also installed approximately 0.8 m deeper in the ground compared to the other

Table 5. Comparison between measured properties of excavated pipes and required values for new PVC sewer pipes given in NEN-EN 1401-1.

		Mean measured value								
Property	Required value (NEN-EN 1401-1)	A-1	A-2	A-3	A-4	B-1	B-2	B-3	B-4	R
PVC content (%)[a]	≥80	78.9	81.6	82.1	80.5	84.7	83.2	82.8	73.6	80.4
Density (g/cm^3)	1.35 ≤ density ≤ 1.6	1.42	1.41	1.41	1.41	1.41	1.41	1.41	1.49	1.41
Processing temperature (°C)[b]	≥185	174.1	169.3	174.7	175.1	179.8	179.9	185.7	192.4	185.7
Strain at break (%)	≥80[c]	–	–	–	–	136.9	175.3	53.3	24.5	212.0

[a]This parameter is obtained via Thermogravimetric Analysis (TGA).
[b]This parameter is obtained via Differential Scanning Calorimetry (DSC).
[c]This value is given for tensile tests performed at 23 ± 2 °C

Figure 9. In-situ footage after excavation of pipes A-3 (left) and B-2 (middle) with break due to third party impact, and pipe B-3 (right) with crack due to poor installation quality.

tested pipes and under a paved street, increasing the vertical load at the crown of the pipe. The combined effect of soil conditions and the low bending stiffness of plastic pipes could lead to such pre-buckling conditions (Stein, 2001).

In case of pipe A-3, no sharp object (e.g. rock) was found to be in contact with the pipe near the break, while deep scratches were observed in the deformed area above the defect (Figure 9, left). Based on this fact, it can be safely assumed that this defect is caused by human activity, conceivably third-party impact. A more evident indication of a similar situation was provided via visual examination of the break at pipe B-2, as the footprint of an excavator's bucket was recognized on the pipe (Figure 9, middle). The likelihood of such a failure cause was increased by the existence of several installed pipes destined for other purposes close to the affected one, hinting at extensive digging activity during the service life of the pipe under consideration.

The source of pipe B-3 failure could be traced back to the installation of the pipe. The crack detected via the inspection was found to be initiated at the contact point between the affected pipe and the concrete protection of a warm water distribution pipe. Nonetheless, the interaction of these two types of infrastructure was trivial compared to the installation practice, as an extra piece of pipe was found around the cracked part of the pipe (Figure 9, right). This fact revealed the human interference regarding the failure and the poor installation quality.

Finally, visual inspection of pipe A-4 revealed that only the inside layer of the bottom of the pipe was cracked; hence no exfiltration of sewage occurred during operation. This crack was apparently formed by the combination of deflection and the fact that pipes with void core demonstrated lower flexural modulus values. Pipe ovalization results in high tensile stresses at the 6 and 12 o' clock position of the inner surface, justifying the crack location.

5. Conclusions

Exhumation and comprehensive testing of 8 PVC sewer pipes (exposed to 16–43 service years) with known defects (fissures, breaks, root intrusion) revealed factors that affect the pipe's operational lifetime. Physical ageing was the most profound mechanism, resulting in an increase in ultimate tensile and flexural stresses followed by lower levels of ductility compared to a brand-new pipe. However, such a comparison can be only indicative given the polydispersity of PVC material and the updated production process.

One critical factor for premature failures was the existence of inherent defects. Especially the incorporation of a recycled or foamed core within the pipe acted as numerous inherent defects, while the core itself reduced significantly the strength and toughness of the pipe. This reduction could imply that excessive pipe bending or deflection is a potential threat to the longevity of the system. However, flexural testing showed that the investigated pipes could bare excessive bending, although pipes with an embedded void core had a comparatively lower flexural modulus.

There was a slight indication that oxidation on the external surface of the pipes had commenced. Signs of discolorization which could suggest potential chemical degradation were also limited to the pipe surface level only. Comprehensive testing led to the conclusion that alterations in properties among pipes originate from different production procedures, rather than a modified molecular structure or chain scission.

This study identified that the most important cause of failure for the examined pipes is related to poor installation quality and human activities. Such activities include excavation in the surroundings of the pipe, most likely due to installation or maintenance of other underground infrastructure. Therefore, it is inadequate to develop sewer asset management strategies based only on the age of the pipe and the pipe material properties. Incorporation of detailed protocols for handling and construction, close supervision during construction and measures against third party impacts are a precondition for long-lasting sewer pipelines.

Acknowledgments

The authors would like to explicitly thank the municipalities of Almere and Breda for providing the tested material. They would also like to thank Armand Middeldorp, Durga Mainali, Gertjan Mulder, Mohammed Jafar and Ruud Hendrikx from TU Delft for their technical support during the experiments. This research is conducted under the “Kennisprogramma Urban Drainage” (Knowledge Programme Urban Drainage). The involved parties are: ARCADIS, Deltares, Gemeente Almere, Gemeente Breda, Gemeente ’s-Gravenhage, Gemeentewerken Rotterdam, Gemeente Utrecht, GMB Rioleringstechniek, KWR Watercycle Research Institute, Platform Water Vallei en Eem, Royal HaskoningDHV, Stichting RIONED, STOWA, Sweco Nederland, Tauw, vandervalk + degroot, Waterboard De Dommel, Waternet and Witteveen + Bos.

Disclosure statement

No potential conflict of interest was reported by the authors.

ORCID

François H. L. R. Clemens http://orcid.org/0000-0002-5731-0582

References

Alferink, F., Guldback, E., & Grootook, J. (1995). *Old PVC gravity sewer pipes: Long term performance*. Proceedings of the 9th International Conference on Plastics Pipes, Edinburgh, Scotland, UK.

Anders, U. (2014). *Highlights on PVC stabilization for pipes – Comparison and trends*. Proceedings of the 17th International Conference on Plastics Pipes, Chicago, USA.

Arsénio, A. M. (2013). *Lifetime prediction of PVC push-fit joints* (Doctoral dissertation). Delft University of Technology, Delft, The Netherlands. Retrieved from doi:10.4233/uuid:18a79a31-abd9-4f24-81f5-15935e3523d0

ASTM D2857-16. (2016). *Standard practice for dilute solution viscosity of polymers*. West Conshohocken, PA: ASTM International.

ASTM D6272-17. (2017). *Standard test method for flexural properties of unreinforced and reinforced plastics and electrical insulating materials by four-point bending*. West Conshohocken, PA: ASTM International.

Bauer, D. (1990). 15 year old polyvinyl chloride (PVC) sewer pipe; A durability and performance review. In G. Buczala & M. Cassady (Eds.), *STP1093-EB buried plastic pipe technology* (pp. 393–401). West Conshohocken, PA: ASTM International. doi:10.1520/STP42134S

Bishop, R. (1990). Retention of pipe stiffness for polyvinyl chloride (PVC) pipe samples exposed to various environments and constant strain. In G. Buczala & M. Cassady (Eds.), *STP1093-EB buried plastic pipe technology* (pp. 7–20). West Conshohocken, PA: ASTM International. doi:10.1520/STP42110S

Cardarelli, F. (2008). Polymers and elastomers. In F. Cardarelli, Materials handbook: A Concise Desktop Reference (2nd ed.) (pp.691–750). London: Springer. doi:10.1007/978-1-84628-669-8_11

Dirksen, J., Clemens, F. H.L.R., Korving, H., Cherqui, F., Le Gauffre, P., Ertl, T., Plihal, H., Müller, K., & Snaterse, C. T.M. (2013). The consistency of visual sewer inspection data. *Structure and Infrastructure Engineering*, *9*(3), 214–228. doi:10.1080/15732479.2010.541265

Folkman, S. (2014). *Validation of the long life of PVC pipes*. Proceedings of the 17th International Conference on Plastics Pipes, Chicago, USA.

Fumire, J. (2008). *Resistance of PVC pipes against disinfectants*. Proceedings of the 14th International Conference on Plastics Pipes, Budapest, Hungary.

Gramann, P., Cruz, J., & Ralston, B. (2010). Using differential scanning calorimetry to determine the quality of a PVC part. *The Madison Group*, 1–6. Retrieved from http://www.madisongroup.com/publications/UsingDSCtoDeterminetheQualityofPVC1.pdf.

Hamid, S. H., Amin, M. B., Maadhah, A. G., & Al-Jarallah, A. M. (1992). Polymer lifetime studies in hostile environments. *Journal of Vinyl and Additive Technology*, *14*(4), 182–186. doi:10.1002/vnl.730140404

Hawkins, T. W., & Mass, T. R. (1994). The effects of sulfuric acid on calcium carbonate filled PVC sewer pipe compounds. In D. Eckstein (Ed.), *STP1222 buried plastic pipe technology* (Vol. 2, 167–179). Philadelphia, PA: ASTM.

Hutchinson, J. M. (1995). Physical aging of polymers. *Progress in Polymer Science*, *20*(4), 703–760. doi:10.1016/0079-6700(94)00001-I

ISO 11358-1. (2014). Plastics – Thermogravimetry (TG) of polymers – Part 1: General principles.

ISO 1183-1. (2012). Plastics – Methods for determining the density of non-cellular plastics – Part 1: Immersion method, liquid pyknometer and titration method.

ISO 18373-1. (2007). Rigid PVC pipes – Differential scanning calorimetry (DSC) method – Part 1: Measurement of the processing temperature.

ISO 6259-2. (1997). Thermoplastics pipes - Determination of tensile properties - Part 2: Pipes made of unplasticized poly(vinyl chloride) (PVC-U), chlorinated poly (vinyl chloride) (PVC-C) and high-impact poly (vinyl chloride) (PVC-HI).

ISO 9969. (2016). Thermoplastic pipes – Determination of ring stiffness.

Jakubowicz, I., & Möller, K. (1992). An FTIR, impact strength and thermal analysis investigation of a PVC window frame naturally aged for 20 years. *Polymer Degradation and Stability*, *36*(2), 111–120. doi:10.1016/0141-3910(92)90146-V

Kowalska, B., Rudawska, A., & Kowalski, D. (2014). Tests on a polyvinyl chloride pipe from an existing water distribution system. *WIT Transactions on the Built Environment*, *139*, 3–14. doi:10.2495/UW140011

Kraemer, E. O. (1938). Molecular weights of celluloses and cellulose derivates. *Industrial & Engineering Chemistry*, *30*(10), 1200–1203. doi:10.1021/ie50346a023

Lasfar, S., Mouallif, I., Latrach, A., Chergui M, H., Choukir, A., & Diab, A. (2014). Resistance of different materials used in sewers systems: Polyvinyl chloride (PVC), polypropylene (PP) and High density polyethylene (HDPE), to sulfuric acid and sodium sulphate attack. *International Journal Engineering Research and Applications*, *42*, 670–678.

Makris, K. F., Langeveld, J., & Clemens, F. H. (2020). A review on the durability of PVC sewer pipes: Research vs. practice. *Structure and Infrastructure Engineering*, *16*(6), 880–817. doi:10.1080/15732479.201973442

Matuana, L.M., Kamdem, D.P., & Zhang, J. (2001). Photoaging and stabilization of rigid PVC/wood-fiber composites. *Journal of Applied Polymer Science*, *80*(11), 1943–1950. doi:10.1002/app.1292
McGarry, F. J., Mandell, J. F., & Hsueh-Lee, L. (2007). Brittle fracture in PVC pipe material. *Journal of Polymer Science: Polymer Symposia*, *72*(1), 83–110. doi:10.1002/polc.5070720116
Meerman, M. (2008). *Lifetime expectancy of PVC-U pipelines for sewer systems*. Proceedings of the 14th International Conference on Plastics Pipes, Budapest, Hungary.
Meijering, T. G., Wolters, M., & Hermkens, R. J. (2004). *The durability of a low-pressure gas distribution system of ductile PVC*. Proceedings of the 12th International Conference on Plastics Pipes, Milan, Italy.
Moser, A., & Folkman, S. (2008). *Buried pipe design* (3rd ed.). New York: McGraw-Hill.
NEN-EN 1401-1. (2019). Plastic piping systems for non-pressure underground drainage and sewerage – Unplasticized poly(vinyl chloride) (PVC-U) – Part 1: Specifications for pipes, fittings and the systems.
Noda, I., Dowrey, A.E., Haynes, J.L., & Marcott, C. (2007). Group frequency assignments for major infrared bands observed in common synthetic polymers. In J. E. Mark (Ed.), *Physical properties of polymers handbook* (pp. 395–406). New York, NY: Springer.
Orwoll, R.A. (2007). Densities, coefficients of thermal expansion, and compressibilities of amorphous polymers. In J. E. Mark (Ed.), *Physical properties of polymers handbook* (pp. 93–101). New York, NY: Springer. doi:10.1007/978-0-387-69002-5_7
Real, L. P., João, I. M., Pimenta, S. I., & Diogo, H. P. (2018). Evaluating the degree of gelation of PVC-U pipes. Comparison of currently available methods. *Polymer Testing*, *70*, 481–485. doi:10.1016/j.polymertesting.2018.08.001
Scholten, F. L., van der Stok, E., Gerets, B., Wenzel, M., & Boege, M. (2016). Residual quality of excavated UPVC gas and water distribution pipelines. Proceedings of the 18th International Conference on Plastics Pipes, Berlin, Germany.
Stanic, N., Langeveld, J. G., & Clemens, F. H. L. R. (2012, September 4–6). *Identification of the information needs for sewer asset management by assessing failure mechanics*. Proceedings of the 9th International Conference on Urban Drainage Modelling, Belgrade, Serbia. IWA.
Stein, D. (2001). *Rehabilitation and maintenance of drains and sewers*. Berlin: Ernst & Sohn.
Stone, S. L., Dzuray, E. J., Meisegeier, D., Dahlborg, A., Erickson, M., & Tafuri, A. N. (2002). *Decision-support tools for predicting the performance of water distribution and wastewater collection systems*. Cincinnati, OH: US Environmental Protection Agency, Office of Research and Development.
Visser, H. A., Bor, T. C., Wolters, M., Warnet, L. L., & Govaert, L. E. (2011). Influence of physical aging on impact embrittlement of uPVC pipes. *Plastics, Rubber and Composites*, *40*(5), 201–212. doi:10.1179/1743289810Y.0000000021
Weller, J., Hermkens, R.J.M., & Van der Stok, E.J.W. (2016). *Residual quality of the PVC gas grid – results of 10 years of on-going research*. Proceedings of the 18th International Conference on Plastics Pipes, Berlin, Germany.
Whittle, A. J., & Tennakoon, J. (2005). Predicting the residual life of PVC sewer pipes. *Plastics, Rubber and Composites*, *34*(7), 311–317. doi:10.1179/174328905X59773
Wilkes, C. E., Summers, J. W., Daniels, C. A., & Berard, M. T. (2005). *PVC handbook*. Munich: Hanser.
Wypych, G. (2015). *PVC degradation and stabilization*. Toronto, Canada: ChemTec Publishing. doi:10.1016/C2014-0-01988-0

Appendix

Uncertainty in viscosity measurements

Uncertainty exists in all types of measurements. However, it is expected to be significant in viscosity measurements, as several steps are incorporated, each of which has its own uncertainty propagating through the final outcome. Application of the law of uncertainty propagation to Equation (1) yields the uncertainty of inherent viscosity (Equation (A1)), assuming independent measurements each having a Gaussian uncertainty:

$$\delta_{\eta_{inh}} = \sqrt{\left(\frac{\partial \eta_{inh}}{\partial \eta}\delta_\eta\right)^2 + \left(\frac{\partial \eta_{inh}}{\partial \eta_o}\delta_{\eta_o}\right)^2 + \left(\frac{\partial \eta_{inh}}{\partial c}\delta_c\right)^2} = \sqrt{\frac{1}{(\eta \cdot c)^2}\delta_\eta^2 + \frac{1}{(\eta_o \cdot c)^2}\delta_{\eta_o}^2 + \frac{\left(\ln\frac{\eta}{\eta_o}\right)^2}{c^4}\delta_c^2} \tag{A1}$$

where $\delta_{\eta_{inh}}$ is the uncertainty of the inherent viscosity (mL/g), δ_η is the uncertainty of the polymer solution's viscosity (Pa·s), δ_{η_o} is the uncertainty of the solver's viscosity (Pa·s), and δ_c is the uncertainty of the polymer solution concentration (g/mL).

Similarly, the uncertainty of the polymer solution concentration was estimated via:

$$\delta_c = \sqrt{\left(\frac{\partial c}{\partial M}\delta_M\right)^2 + \left(\frac{\partial c}{\partial V}\delta_V\right)^2} = \sqrt{\frac{1}{V^2}\delta_M^2 + \frac{M^2}{V^4}\delta_V^2} \tag{A2}$$

where M is the mass of the pipe sample (g) with its respective uncertainty δ_M, and V is the volume of the solver (mL) with its respective uncertainty δ_V. Uncertainty δ_M is considered as the last significant digit of the used balance (10^{-4}g) and δ_V is the standard error of the used pipette (0.02 mL). Uncertainties δ_η and δ_{η_o} were estimated as the standard deviation of 10 runs of the exact same procedure with the same solution (Figure A1). Subsequently, the shear rates with the lower uncertainties were considered in Equation (3) (i.e. 38, 76, 115, 154, 193 and 231 s^{-1}).

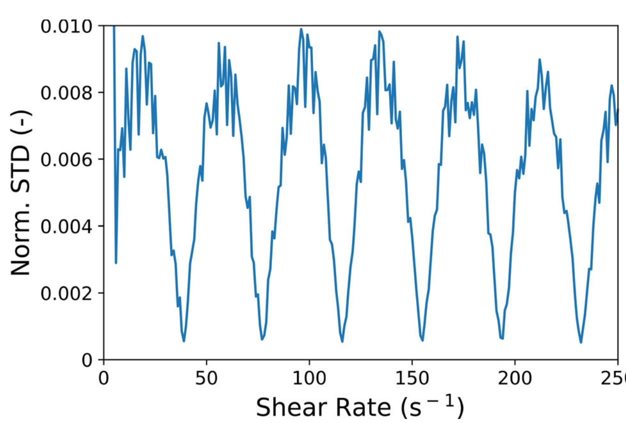

Figure A1. Normalized Standard Deviation (STD) with respect to shear rate obtained by 10 consecutive measurements on cyclohexanone at 20 °C with Anton-Paar 302. The same method utilized for viscosity measurements of the investigated polymer solutions was applied.

Mechanical properties

The detailed tensile and flexural properties of the tested pipe samples are summarized in Table A1.

Table A1. Mechanical properties of examined PVC samples derived by tensile (24 ± 2 °C) and 4-point bending testing (20 ± 0.2 °C).

Sample	Tensile modulus (GPa)	Ultimate stress (MPa)	Stress at break (MPa)	Elongation at break (%)	Flexural modulus (GPa)	Ultimate flexural stress (MPa)
A-1	–	–	–	–	3.24 ± 0.02	87.7 ± 1.5
A-2	–	–	–	–	3.33 ± 0.07	88.7 ± 0.2
A-3	–	–	–	–	2.92 ± 0.10	79.6 ± 1.3
A-4	–	–	–	–	2.98 ± 0.12	83.0 ± 3.3
B-1	3.09 ± 0.02	54.3 ± 2.1	44.2 ± 3.8	136.9 ± 44.1	3.33 ± 0.74	89.5 ± 13.0
B-2	2.69 ± 0.30	53.2 ± 0.3	49.8 ± 1.8	175.3 ± 20.1	*	*
B-3	2.32 ± 0.15	47.8 ± 1.7	36.2 ± 0.2	53.3 ± 16.8	3.34 ± 0.04	84.1 ± 0.7
B-4	1.37 ± 0.07	28.9 ± 1.2	24.1 ± 0.7	24.5 ± 9.6	3.32 ± 0.07	70.4 ± 2.2
R	2.25 ± 0.19	49.3 ± 0.2	50.8 ± 2.3	212.0 ± 27.0	3.17 ± 0.01	80.7 ± 1.1

*Material was inadequate for specimen preparation.